Journal of
Proteomics & Bioinformatics

Zanatta et al., J Proteomics Bioinform 2012, 5:7
DOI: 10.4172/jpb.1000229

Research Article Open Access

Quantum Biochemistry Description of the Human Dopamine D3 Receptor in Complex with the Selective Antagonist Eticlopride

Geancarlo Zanatta[1]*, Ito L. Barroso-Neto[2], Victorio Bambini-Junior[1], Mellanie F. Dutra[1], Eveline M. Bezerra[3], Roner F. da Costa[4], Ewerton W. S. Caetano[5], Benildo S. Cavada[2], Valder N. Freire[4] and Carmem Gottfried[1]

[1]*Department of Biochemistry at Federal University of Rio Grande do Sul, 90035-003 Porto Alegre, RS, Brazil*
[2]*Department of Biochemistry at Federal University of Ceará, 60455-760 Fortaleza, CE, Brazil*
[3]*Post-graduate Program in Pharmaceutical Sciences, Pharmacy Faculty, Federal University of Ceará, 60430-372 Fortaleza, CE, Brazil*
[4]*Department of Physics at Federal University of Ceará, 60455-760 Fortaleza, CE, Brazil*
[5]*Federal Institute of Education, Science and Technology, 60040-531 Fortaleza, CE, Brazil*

Abstract

In the quest to improve the treatment of Parkinson´s disease and Schizophrenia, one of the proposed strategies has been the development of subtype selective ligands targeting D_2 and D_3 dopamine receptors. An essential advance for this type of strategy was the recent crystallographic elucidation of the human dopamine D_3 receptor structure in complex with the antagonist eticlopride, revealing important features of the ligand-binding pocket. Taking this data into account, we have performed a quantum biochemistry investigation of the eticlopride binding to D_3 in order to understand the implications and the individual contribution of amino acid residues at the binding pocket. The contribution of the residues were evaluated using the molecular fractionation with conjugate caps approach and binding energies calculated within the framework of the density functional theory using both the local density and generalized gradient approximations. The simulations show that the total interaction energy of eticlopride bound to D_3 stabilizes only for a pocket radius of at least 8.0Å. The strongest estimated drug-residue interaction energy was observed for Asp110 followed, among others, by Phe345, Phe346, Ile183, Val107, Tyr373, Val189, Trp342, Cys114 and Val82 hydrogen and van der Waals bonds, the later being a repelling residue which was not considered to be important in the original crystallographic data analysis. Our results highlight the key amino acid residues involved in the binding of antipsychotics to D3R and collaborate to a potential further analysis with regard to the binding of different antagonists in members of the dopamine receptor family.

Keywords: Quantum biochemistry; Dopamine receptor; Eticlopride; D3 binding pocket; Quantum mechanics; DFT; Antipsychotic; *Ab initio*

Introduction

Dopamine is a fundamental neurotransmitter associated with fine movement coordination, cognition, emotion, affect, memory and the reward pathway. Impairments in its metabolism lead to severe disorders such as Parkinson's disease and schizophrenia [1-7]. Dopamine receptors belong to the G protein-coupled receptor (GPCR) family and are classified into two subfamilies: D1-like receptors (D1 and D5), which activate adenylyl cyclase through the stimulatory G-protein alpha subunit, and D2-like receptors (D2, D3 and D4) coupled to the inhibitory G-protein alpha subunit with inhibitory effect over adenylyl cyclase [8,9]. Due to alternative splicing events during the maturation of the receptor pre-mRNA and gene polymorphism, more than five different receptors can be observed and among them, two forms of D2 receptors (D2R) [10].

It is postulated that many antipsychotics exert their therapeutic effects through the blockage of dopamine receptors [11,12]. According to the binding profile, side effect events and mechanisms of action, antipsychotics are classified as typical or atypical [11-13]. Typical antipsychotics block D2R in the mesolimbic and nigrostriatal pathway leading to extrapyramidal symptoms (EPS) and tardive dyskinesia, while atypical antipsychotics are associated with fewer side effects [12]. Two hypothesis are frequently used to explain this phenomena: (i) the dopamine receptor blockade in the nigrostriatal pathway is reversed by serotonin receptor blockade [14,15]; (ii) atypical agents have fast dissociation from the dopamine receptor, lasting only long enough to cause antipsychotic action, but not long enough to cause the side effects associated with typical agents [13].

The focus of this work is on eticlopride, ($C_{17}H_{25}ClN_2O_3$), 2S(–)-3-chloro-5-ethyl-N-[(1-ethyl-2-pyrrolidinyl)methyl]-6-hydroxy-2-methoxybenzamide, which is a substituted benzamide analog with high affinity and selectivity for D2-like receptors that was initially developed as a potential antipsychotic agent [16]. A great deal of research has utilized this drug to understand better the central dopamine receptor function, the role of D2-like receptors in behavior, and the influence of blockade of these receptors on several preclinical animal models. While eticlopride is not used clinically, it remains a viable research tool for understanding dopamine receptor function and behavior [16].

Recently, the resolved structure at 3.15Å of the human dopamine D3 receptor (D3R) co-crystallized with the antagonist eticlopride, a potent D2R/D3R antagonist, has been published PDB ID: 3PBL [17]. The high degree of homology between D3R and D2R, especially in the binding pocket, makes this structure a key tool to study, at the molecular level, the mechanisms surrounding the interactions of agonists and antagonists with the receptor, the stabilization of the binding energy and the structural determinants of receptor specificities. Additionally,

***Corresponding author:** Geancarlo Zanatta, Departamento de Bioquímica, Rua Ramiro Barcelos, 2600 – anexo, Bairro Santa Cecília 90035-000 - Porto Alegre – RS, Brazil, Tel: +55 51 3308-3570 / 3308-5551; E-mail: geancarlo.zanatta@gmail.com

Received June 05, 2012; **Accepted** July 24, 2012; **Published** July 27, 2012

Citation: Zanatta G, Barroso-Neto IL, Bambini-Junior V, Dutra MF, Bezerra EM, et al. (2012) Quantum Biochemistry Description of the Human Dopamine D3 Receptor in Complex with the Selective Antagonist Eticlopride. J Proteomics Bioinform 5: 155-162. doi:10.4172/jpb.1000229

information from eticlopride contact residues at the pocket side is remarkable as it is known that it have a greater affinity to D2R over D3R and no affinity for D1R [16,17]. The crystal structure of the human D3R provides an opportunity to identify subtle structural differences, at the molecular level, between closely related GPCRs that can be exploited for novel drug design [17]. On the other hand, a DOCK2010 participation involved in the blind prediction of the dopaminergic D3 receptor in complex with the D2/D3 selective antagonist eticlopride, succeeded in producing a correctly predicted eticlopride-D3 receptor complex out of three submitted models [18].

The use of quantum *ab initio* simulations commonly applied in chemistry to investigate biological systems at the molecular level is very tempting. However, it demands a high computational cost due to the very large number of electrons involved. One way to overcome this difficulty is to describe the system by using the electronic density ρ(r), which depends on three space coordinates only, instead of the wave function, which changes on the 3N space coordinates (N being the number of electrons). Such is the essential feature of Density Functional Theory (DFT), where the total energy of a multielectronic system is expressed as a functional of the electron charge density, which is found after solving the Kohn-Sham equations [19,20]. Another important approach to work through quantum mechanics calculations on large molecules or molecular systems is the use of fragmentation methods to make it more computationally acceptable and, at the same time, maintain the good accuracy of the quantum calculation [21]. The Molecular Fractionation with Conjugate Caps (MFCC) methods is a useful approach to calculate interaction energies for protein-ligand systems. In this method, the peptide bonds of the protein are fragmented and the bonds are capped with portions of the neighboring amino-acid residues of the molecule in order to resemble the local environment [21-25].

In this context, a detailed understanding of the eticlopride bonding to each D3R residue in the binding pocket by quantum biochemistry methods [26] is essential for its energetic description and also to determine the individual contributions to the total binding energy. In addition, this approach may contribute to the molecular structure improvement and/or to the design of new antipsychotic drugs. As emphasized by Zhou et al. [27], quantum mechanical (QM) methods are becoming popular in computational drug´s design and development, mainly because high accuracy is required to estimate (relative) binding affinities. According to Raha et al. [28], the routine use of QM methods in all phases of *in silico* drug design is of upmost importance for the evolution of this field. Recent works in our group have employed quantum approaches combined with classical molecular dynamics to predict the adsorption of ascorbic acid on the C60 fullerene and suggested the use of this formulation to act against the oxidative effect of C60 [29]. Also, using this approach, it was possible to predict the theoretical absorption levels of ibuprofen on C60 fullerene seeking its transdermal delivery [30]. Moreover, the effectiveness of drug inhibition of HMG-CoA redutase using quantum biochemistry computations were predicted by comparing the binding energy profile of different statins [31]. QM methods can also be used locally to improve crystal structures [24]. While quantum refinement is computationally expensive if compared with standard crystal structure refinement techniques, it may become a standard tool, as the computers are becoming faster and cheaper, especially when the refined site is of major interest [24].

The purpose of this work is to present an improved description of the eticlopride binding to D3R through a quantum biochemistry investigation of their interaction with close residues inside binding pockets of varying radii. The individual contribution of amino acid residues involved in D3R-eticlopride binding was calculated using the X-ray structure of the D3R co-crystalized with eticlopride [17]. The present study highlights the significant energy contribution of Asp110, and demonstrated for the first time the participation of Val107, Ser182, Phe188, Val82 and Asn185 on the binding of eticlopride to D3.

Materials and Methods

Structural data

The calculations performed during this study took advantage of the X-ray crystal structure of human dopamine D3 receptor in complex with eticlopride (PDB ID: 3PBL) determined with a resolution of 3.15Å. The crystal asymmetric unit contains two receptors (A and B) in an antiparallel orientation, both exhibiting slight differences in shape. Thus, we arbitrarily chose the receptor A to use as a model of study. All residues of amino acids within a radius up to 10Å from the centroid of eticlopride were taken into account. The protonation state of eticlopride at physiological pH was obtained using the Marvin Sketch code version 5.4.1.0 (Marvin Beans Suite– ChemAxon). The crystallographic structure modification was performed by adding a single hydrogen atom into the amine group at the ethyl-pyrrolidine ring of eticlopride followed by the charging setup to +1 (electron charge =-1).

Classical and DFT calculations

Hydrogen atoms were inserted into the D3 X-ray structure and their positions were optimized classically, keeping the other atoms frozen. The optimization procedure was performed using the Forcite code with convergence tolerances set to 2.0×10^{-5} kcal•mol^{-1} (total energy variation), 0.001 kcal•mol^{-1}Å^{-1} (maximum force per atom) and 1.0×10^{-5}Å (maximum atomic displacement).

Calculations at DFT level, using the DMOL3 code [32,33], were performed using: 1) the Local Density Approximation (LDA) for the exchange-correlation functional with PWC parameterization, and 2) the Generalized Gradient Approximation (GGA) with PBE parameterization. The DNP numerical basis set was adopted to expand the Kohn-Sham orbital for all electrons. The orbital cutoff, which is a parameter used to control the quality of the numerical basis set and the numerical integrations performed during the computations was set to 3.7Å. This cutoff serves to reduce computation time with little impact on the accuracy of the results and is a very fine value for the atoms involved in the system under study. The total energy variation, which specifies the self-consistent field (SCF) convergence threshold, was selected to be 10^{-6} Ha, ensuring a well converged electronic structure for the system.

Molecular fractionation with conjugate caps (MFCC)

The MFCC scheme is a very useful approach to achieve an accurate description of biological systems through quantum calculations [21-25]. To avoid missing important amino acid residue interactions, all amino acid residues within an increasing radius from the centroid of eticlopride were took into account until energy convergence has been achieved (see "Energy stabilization versus residue distance to the centroid", below). The set of chosen amino acid residues were used to form individual sets of capped fragments, including disulfide concaps when necessary (Figure 1). The eticlopride molecule is represented by M and R^i is the i-th amino acid residue interacting with M. The C^{i-1}

(C^{i+1}) cap is made from the residue covalently bound to the amine (carboxyl) group of R^i with hydrogen atoms added wherever necessary to passivate the dangling bonds.

The interaction (binding) energy between the eticlopride molecule M and each amino acid residue R^i, E(M-R^i), is calculated at DFT level [32,33], according to:

$$E(M\text{-}R^i) = E(M\text{-}C^{i-1}R^iC^{i+1}) - E(C^{i-1}R^iC^{i+1}) - E(M\text{-}C^{i-1}C^{i+1}) + E(C^{i-1}C^{i+1}) \quad (1)$$

At the right side of Eq. (1), the first term E(M-$C^{i-1}R^iC^{i+1}$) is the total energy of the system formed by the eticlopride and the capped residue; the second term, E($C^{i-1}R^iC^{i+1}$), gives the total energy of the capped residue alone, while the third term, E(M-$C^{i-1}C^{i+1}$) is the total energy of the system formed by the set of caps and M; finally, E($C^{i-1}C^{i+1}$) is the total energy of the system formed by the isolated caps.

The BIRD Panel

The energies of individual amino acid residues are plotted into the panel BIRD (Binding site, Interaction energy and Residues Domain), which shows clearly: (i) the binding energy (in kcal•mol^{-1}) of the drug to each residue at the binding site depicted using horizontal bars, from which one can assess quantitatively the relevance of each residue at the binding site, whether attracting or repelling the drug; (ii) the most important residues contributing to the binding, which are shown in the column of residues in the left side; (iii) the region i, ii or iii of eticlopride closer to each residue; and (iv) the radius distance of each residue to the eticlopride centroid, as given in the right side. The total binding energy was obtained by adding up the individual contribution of each residue.

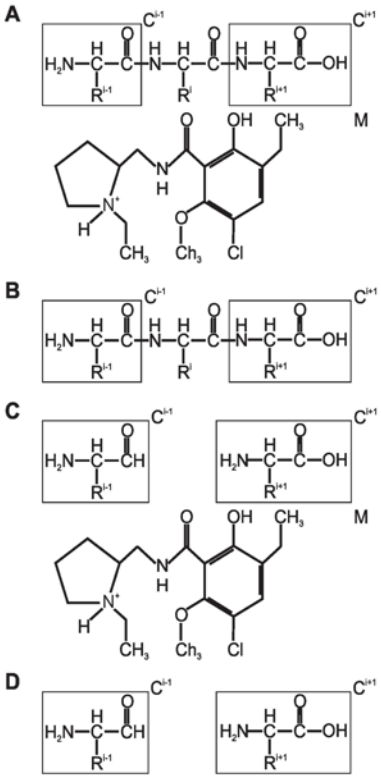

Figure 1: MFCC scheme showing four distinct fragment systems employed in the present study: (A) etilclopride plus amino acid residue with conjugated caps; (B) amino acid residue with conjugated caps; (C) eticlopride plus conjugated caps; (D) conjugated caps only.

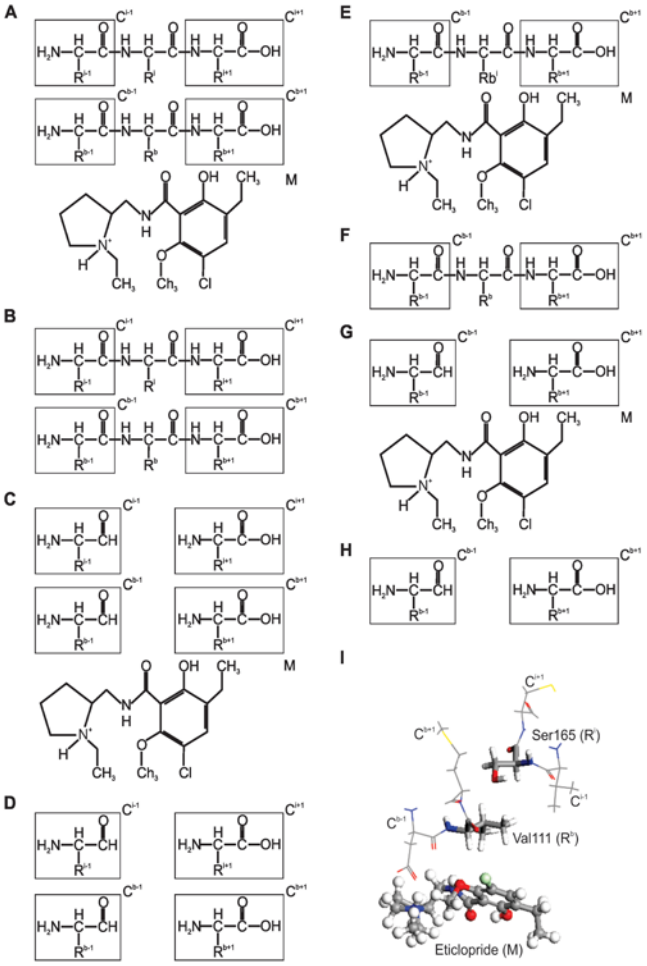

Figure 2: Shielding effect and the MFCC scheme showing eight distinct fragment systems employed in the present study: (A) etilclopride, analyzed residue and shielding residue with conjugated caps; (B) analyzed residue and shielding residue with conjugated caps; (C) eticlopride plus conjugated caps; (D) conjugated caps only; (E) eticlopride plus shielding amino acid residue with conjugated caps; (F) shielding residue with conjugated caps; (G) eticlopride plus conjugated caps; (H) conjugated caps only; (I) representative image of shielding effect of Val111 over Ser165 interaction with eticlopride. Eticlopride, analyzed residue, shielding residue and caps are represented as M, R^i, R^b and C, respectively.

Shielding effect

The shielding effect decreases the attraction between the R^i residue and the eticlopride molecule M and is due to the presence of neighbour residues (R^b) placed between eticlopride and R^i. In this situation, the interaction (binding) energy E(M-R^i) is calculated in two steps (Figure 2). First, the energy, taking in to account both the R^b and R^i contributions, E(M-R^{i+b}), is obtained:

$$E(M\text{-}R^{i+b}) = E(M\text{-}C^{i-1}R^iC^{i+1}\ C^{b-1}R^bC^{b+1}) - E(C^{i-1}R^iC^{i+1}\ C^{b-1}R^bC^{b+1}) - E(M\text{-}C^{i-1}C^{i+1}\ C^{b-1}C^{b+1}) + E(C^{i-1}C^{i+1}\ C^{b-1}C^{b+1}) \quad (2)$$

Secondly, the E(M-R^b) energy contribution is calculated:

$$E(M\text{-}R^b) = E(M\text{-}C^{b-1}R^bC^{b+1}) - E(C^{b-1}R^bC^{b+1}) - E(M\text{-}C^{b-1}C^{b+1}) + E(C^{b-1}C^{b+1}) \quad (3)$$

Finally, the corresponding individual interaction (binding) energy E(M-R^i) is obtained according to:

$$E(M\text{-}R^{i}) = E(M\text{-}R^{i+b}) - E(M\text{-}R^{b}) \quad (4)$$

Energy stabilization versus residue distance to the centroid

To avoid using an arbitrary binding pocket size which could risk missing residues with important contributions to the binding energy, the binding radius was varied until the total binding energy variation was very small. The total binding energy as a function of the binding site radius was obtained for a 2.5-10Å radius range with increasing steps of 0.5Å (only residues with at least one atom inside an imaginary sphere centered at the drug centroid were taken into account to compute the total binding energy). The converged binding pocket radius was achieved when the variation of the total binding energy was smaller than 10% after a radius size increase by 2Å.

Results

In order to best mimic the physiologic conditions, an eticlopride molecule structure was assessed at pH 7.2 and showed protonation at the amine group of the pyrrolidine region. Protonated etilcopride with numbered atoms is shown in Figure 3-A, and its electron density onto an electrostatic potential isosurface is represented in Figure 3-B.

To investigate the binding mechanism of eticlopride, hydrogen atoms were added to the D3 receptor-eticlopride crystallographic structure (receptor-eticlopride) and their positioning was optimized to minimize the total energy. This procedure generated a new structure with shorter distances among residues and eticlopride (Table 1).

Afterwards, to ensure that all relevant residues were included into the QM analysis, the dependence of the total binding energy on the binding site radius (measured from the etilclopride centroid) was assessed (Figure 4). According to our simulations, interaction energy stabilization was achieved for a binding site radius of 8.0Å (nineteen residues included, LDA: -259.21 kcal•mol^{-1}; GGA: -171.48 kcal•mol^{-1}), with no significant change for a radius up to 10Å (LDA: -266.56 kcal•mol^{-1}; GGA: -182.24 kcal•mol^{-1}). The most important residues within 8.0Å are: Phe345, Ile183, Asp110, His349, Trp342, Tyr365, Val111, Val107, Thr369, Phe346, Tyr373, Cys114, Ser182, Val189, Leu168, Phe106, Phe188, Ser192 and Val82.

The complete list of individual energy contribution of 42 residues (using LDA and GGA approximations) as well as the distance to the eticlopride centroid are depicted in Table 2. Among them, twenty contribute significantly to the total binding energy as shown in the

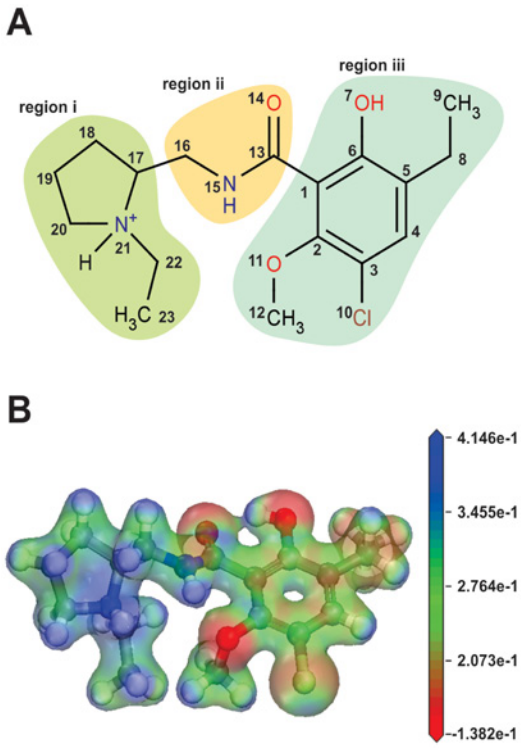

Figure 3: Eticlopride molecule. (A) Chemical structure with atoms labeled. Region i represents the pyrrolidine moiety with the tertiary amine protonated, as observed at physiological pH; region ii represents the amide group; and region iii the aromatic moiety with substituents. (B) Electron density projected onto an electrostatic potential isosurface showing negatively charged regions in red and positively charged regions in blue.

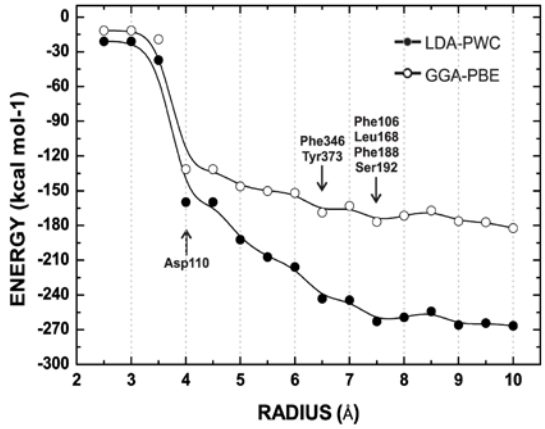

Figure 4: Behavior of the total interaction energy as a function of the binding pocket radius. When Asp110 is considered in the binding site at 4.0 Å, it produces a sharp decrease of the interaction energy. Total energy binding at 8.0 Å with LDA (GGA) approximation: -266.56 (-182.24) kcal mol^{-1}. The solid lines are guides for the eyes only.

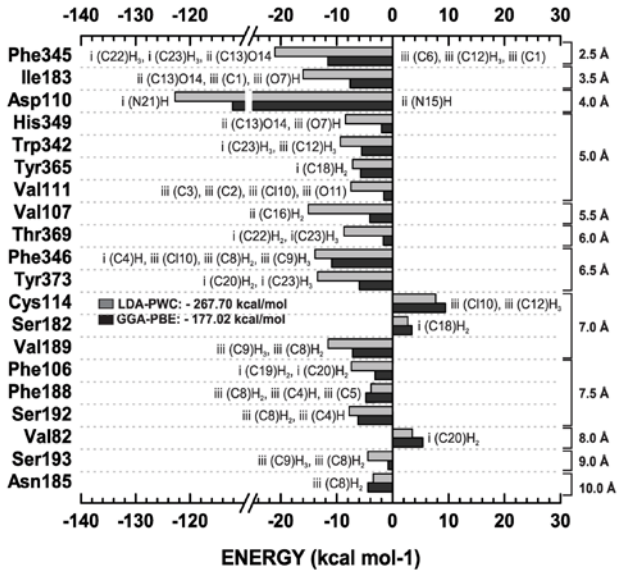

Figure 5: BIRD panel showing the interaction energy (attractive/repulsive) for each amino acid residue. Only residues with interaction energy (LDA or GGA) larger (in absolute value) than 3.0 kcal mol^{-1} are shown.

Residues	Distance(Å)	Eticlopride		Residues	Distance(Å)	Eticlopride	
Asn 185	7.6	iii	$(C8)H_2$	Ser192	2.3	iii	$(C8)H_2$
Asp 110	1.7	i	(N21)H	Ser192	2.6	iii	(C4)H
Asp 110	2.8	ii	(N15)H	Ser193	3.3	iii	$(C8)H_2$
Cys 114	2.6	iii	C110	Ser193	2.3	iii	$(C9)H_3$
Cys 114	3.4	iii	$(C12)H_3$	Ser196	3.1	iii	(C4)H
His 349	3.1	ii	(C13)O14	Ser196	4.0	iii	C110
His 349	2.7	iii	(O7)H	Thr115	4.1	iii	C110
Ile 183	3.1	ii	(C13)O14	Thr369	2.1	i	$(C22)H_2$
Ile 183	2.6	iii	(C1)	Thr369	3.2	i	$(C23)H_3$
Ile 183	2.8	iii	(O7)H	Trp342	2.4	i	$(C23)H_3$
Leu 89	3.7	i	$(C19)H_2$	Trp342	2.9	iii	$(C12)H_3$
Phe 106	2.3	i	$(C19)H_2$	Tyr365	2.7	i	$(C18)H_2$
Phe 106	3.3	i	$(C20)H_2$	Tyr365	3.1	i	(C17)H
Phe 188	4.2	iii	$(C8)H_2$	Tyr373	2.4	i	$(C20)H_2$
Phe 188	5.1	iii	(C4)H	Tyr373	3.4	i	(N21)H
Phe 188	5.0	iii	(C3)	Tyr373	2.6	i	$(C23)H_3$
Phe 345	2.6	i	$(C22)H_2$	Val107	3.8	i	$(C19)H_2$
Phe 345	2.2	ii	(C13)O14	Val107	2.7	ii	$(C16)H_2$
Phe 345	2.8	iii	(O7)H	Val111	2.4	iii	C110
Phe 345	2.9	iii	(C2)	Val111	2.9	iii	O11
Phe 345	3.4	iii	$(C12)H_3$	Val111	2.9	iii	C6
Phe 345	3.1	iii	$(C9)H_3$	Val111	3.1	iii	C5
Phe 346	2.6	iii	(C4)H	Val189	3.1	iii	$(C9)H_3$
Phe 346	3.3	iii	C110	Val189	2.4	iii	$(C8)H_2$
Phe 346	2.6	iii	$(C8)H_2$	Val350	3.1	iii	$(C9)H_3$
Phe 346	2.8	iii	$(C9)H_3$	Val82	4.3	i	$(C20)H_2$
Ser 182	3.6	i	$(C18)H_2$	Val86	3.0	i	$(C20)H_2$
Ser 182	4.4	ii	$(C16)H_2$	Val86	3.3	i	$(C19)H_2$

Table 1: Centroid distances between eticlopride and the amino acid residues at the binding site after inserting and optimizing hydrogen atomic coordinates.

Residue	E_{LDA}	E_{GGA}	Radius	Residue	E_{LDA}	E_{GGA}	Radius
Phe345	-21.04	-11.61	2.5	Thr108	0.90	1.03	8.5
Ile183	-15.99	-7.57	3.5	Val86	0.30	0.27	8.5
Asp110	-122.78	-112.21	4.0	Cys181	-2.68	-2.97	9.0
His349	-8.44	-1.97	5.0	Leu109	-0.83	-0.81	9.0
Trp342	-9.31	-5.53	5.0	Ser165	-2.17	-2.05	9.0
Tyr365	-7.15	-5.72	5.0	Ser184	0.93	0.87	9.0
Val111	-7.47	-1.56	5.0	Ser193	-4.44	-0.83	9.0
Val107	-15.07	-4.08	5.5	Ser196	-0.58	-0.88	9.0
Thr369	-8.70	-1.68	6.0	Thr115	1.19	0.77	9.0
Phe346	-13.87	-10.86	6.5	Thr368	-1.51	-1.85	9.0
Try373	-13.42	-5.94	6.5	Val350	-1.52	-1.52	9.0
Cys114	7.70	9.41	7.0	Met113	1.65	-0.83	9.5
Ser182	2.70	3.40	7.0	Thr353	0.72	0.10	9.5
Val189	-11.55	-7.16	7.0	Val78	-0.68	-0.23	9.5
Leu168	0.63	0.28	7.5	Asn173	-0.99	-1.46	10.0
Phe106	-7.35	-3.13	7.5	Asn185	-3.43	-4.43	10.0
Phe188	-3.85	-4.78	7.5	Asn352	2.70	2.84	10.0
Ser192	-7.77	-6.16	7.5	Leu89	-1.49	-2.00	10.0
Val82	3.52	5.39	8.0	Phe197	0.28	0.44	10.0
Gly372	1.56	1.33	8.5	Thr348	0.04	-0.67	10.0
Met112	2.19	1.85	8.5	Trp370	0.50	0.27	10.0

Table 2: Individual amino acid residue contribution as a function of the radius size. Energies are given in kcal·mol^{-1}. In red, residues pointed as interacting to eticlopride in the crystallographic data; in blue, residues with important contributions to the energy, but not mentioned in the analysis of crystal measurements. LDA and GGA are expressed in kcal·mol^{-1}; radius in Å.

BIRD panel depicted in Figure 5 as follows: Phe345, Ile183, Asp110, His349, Trp342,Tyr365, Val111, Val107, Thr369, Phe346, Tyr373, Cys114, Ser182, Val189, Phe106, Phe188, Ser192, Val82, Ser193, and Asn185.

A classical characteristic of eticlopride is the formation of two pseudo rings: (i) between the carbonyl group (O14) at amide group and the hydroxyl group (O7H) at the aromatic ring; (ii) between the oxygen (O11) at the methoxy group and the hydrogen atom bound to nitrogen (NH15) at amide group. Intramolecular hydrogen bonds were observed after energy minimization procedures and can be observed in Figure 6, where also residues with large energy contribution to eticlopride binding are represented.

The charge distribution in the ligand-binding pocket can be visualized by projecting the charge density onto an electrostatic potential isosurface, as shown in Figure 7 for the LDA data. Looking at it, we see the attractive and repulsive residues at the D3 binding pocket. The carboxylate group of Asp110 exhibits a negative charge density while i(N21)H shows a positive charge density, which explains the relevance of this interaction in the formation of the ionic bridge.

Discussion

The recent crystal structure elucidation of D3R-eticlopride has made it possible to use the structural data of the receptor to predict binding-molecular [17,34]. In this study, we have used *ab initio* computations applying the Molecular Fractionation with the Conjugate Caps (MFCC) [23-25] approach, within the framework of DFT, to evaluate the interaction energy between eticlopride and individual residues in D3 receptor. The results reveal the strength of the drug interaction with each residue in the binding pocket, as well as the behavior of the total interaction energy as a function of the binding pocket size.

Using the hydrogen-optimized structure, further quantum calculations were carried out to obtain a binding energy profile. Different from other approaches, QM methods are practical only for systems with a few hundred of atoms at most due to the computational cost. This limitation has led us to make a compromise in choosing an appropriate range of neighbour residues to be taken into account for the binding energy calculations. Indeed, as pointed out by Hu et al. [35], to assess the relevance of residues based only on their relative positioning can be misleading, as the interaction energy contribution of each residue does not always correlate with distance. In this study, we have fragmented the D3-eticlopride structure using the MFCC approach and the individual contributions of each residue were calculated. This strategy was made to overcome the limitation in the number of atoms and to be able to analyze, via quantum biochemistry, more residues than those previously reported as important in both crystallographic data (contact residues) [17] and modeled structures of the dopamine receptor [34,36].

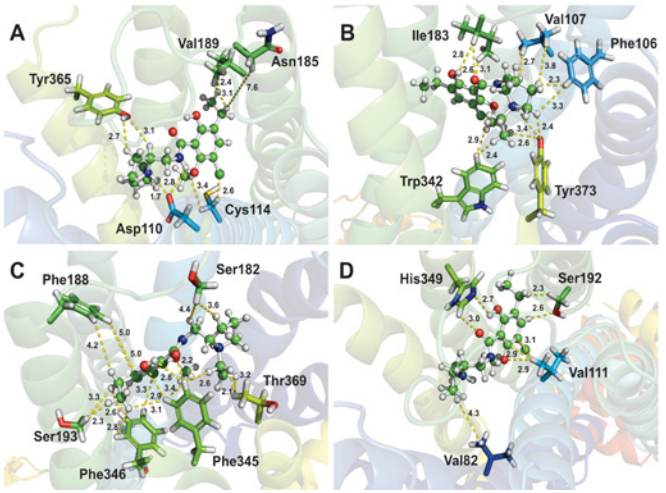

Figure 6: Spatial arrangement of amino acid residues with largest contribution to the binding energy at the binding pocket. (A) Salt bridge between Asp110 side chain and the tertiary amine at pyrrolidine ring. A repulsive interaction with Cys114 is related with the presence of a chloride substituent in the aromatic ring. Orientation of the optimized hydrogen atom in (O7)H in the direction of oxygen in the hydroxyl group (O14) indicates the formation of a pseudoring. (B) Ile183 is the second closest residue to eticlopride and interacts via hydrogen and van der walls bonds. (C) Attractive interactions of Phe345 and Phe346 and repulsive contribution of Ser182. (D) Val82 repels eticlopride probably due to its interaction with region i. Yellow dashed lines show the distance of the most relevant amino acid residues to the closest atoms of eticlopride.

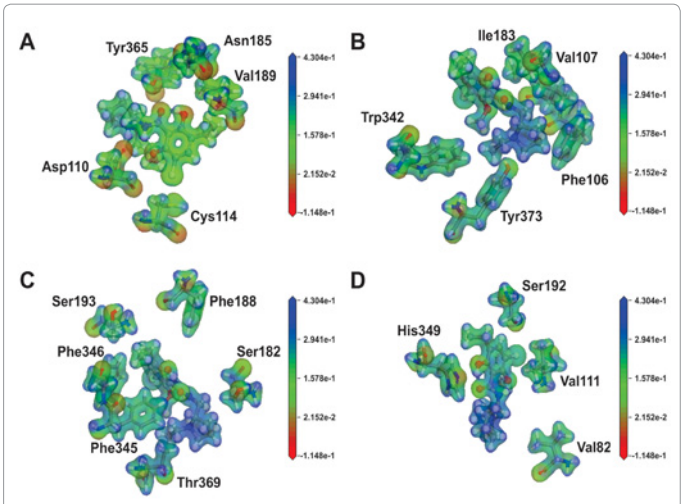

Figure 7: Electrostatic potential isosurfaces. Figure shows projected electron densities for eticlopride interacting with the attractive residues (A) Asp110, Asn185, (B) Ile183, Val107, (C) Phe345, Phe346, Phe188, and with the repulsive residues (A) Cys114, (C) Ser182 and (D) Val82.

After an exhaustive analysis of individual energy contribution of 42 amino acid residues, we have achieved the stabilization of the binding energy at a radius of 8Å from the eticlopride centroid. At this radius distance, nineteen residues give rise to a binding energy of -259.21 (-171.48) kcal•mol^{-1} using LDA (GGA) approximation, only attractive interactions were observed for the residues within 6.5Å, while repulsive interactions were found for larger distances.

As described in previous studies, the Asp110 side chain of TM3, which is pivotal to the binding of aminergic ligands in dopamine receptors [34,36-38], was responsible for the largest contribution through an attractive interaction with the tertiary amine in the ethyl-pyrrolidine ring of eticlopride of -122.78 (-112.21) kcal•mol^{-1}, obtained using LDA (GGA) approximation. This interaction occurs through a 2.8Å salt bridge between the amine group of eticlopride and the carboxylate of Asp110, which has been described as structurally and pharmacologically critical for high-afinity ligand-binding to the aminergetic subfamily of GCPRs [17]. In the same way, a recent study using a docking approach demonstrated the importance of the interaction between the amine group of ligands and the residue Asp110 to the control of the stereospecificity of tetrahydropyrazolopyridines (R) and (S) and the reference phenylpiperazine in the D3R receptor

[39]. Another key component of the eticlopride pharmacophore is a substituted aromatic ring connected to the pyrrolidine by an amide bond that fits tightly within a hydrophobic cavity formed by Phe345 and Phe346 in helix VI; Val189, Ser192, and Ser193 in helix V; and Val111 in helix III, as well as Ile183.

The analysis of our results shows five important residues which were not considered to be relevant in the original crystallographic analysis: Val107, Ser182, Phe188, Val82 and Asn185. Val107 interacts attractively with a LDA (GGA) binding energy of -15.07 (-4.08) kcal•mol^{-1}, to eticlopride regions i and ii. This contribution is much larger than that of Leu89 (LDA: -1.49 kcal mol^{-1}; GGA: -2.00 kcal•mol^{-1}) and larger or equivalent to Phe106, Thr369, Trp342, Tyr365, Tyr373 and Val86. In the opposite way, Ser182 repels eticlopride at region I, with 2.70 (3.40) kcal•mol^{-1} in the LDA (GGA) approximation, overcoming the contribution of Val86. Additionally, Val82, with a LDA (GGA) contribution of 3.52 (5.39) kcal•mol^{-1}also acts by repelling the ligand at region i. Interacting with region iii, Phe188 is located in the hydrophobic region of the binding pocket and contributes through attractive interaction with LDA (GGA) energy of -3.85 (-4.78) kcal•mol^{-1}. This contribution is similar to that of Ser193 and larger than the values observed for Ser196 and Val350. Surprisingly, despite the distance to the etilclopride centroid (8Å), Asn185 contributes with an attractive LDA (GGA) binding energy of -3.43 (-4.43) kcal•mol^{-1}.

Another important result is the formation of two intramolecular hydrogen bonds in the eticlopride molecule. One of them, between the methoxy group at aromatic 2-position and the region ii (NH15) at amide moiety, was described in a previous study, with the formation of a six-membered pseudoring being indicated as a requirement for activity in vitro [40]. The second bond leads to the formation of a pseudoring between (O7)H at aromatic 6-position, and O14 at amide moiety. These two intramolecular hydrogen bonds were already described by quantum mechanical calculations of D2-receptors antagonists [41], and are responsible for stabilizing the planar conformation of eticlopride in the binding pocket, as described in the crystallographic data [17] and docking approaches [18].

The data presented in this study may contribute to efforts in developing reliable models of G protein-coupled receptors structures, as well as to predict their interaction with agonists and antagonists. Recently, Soriano-Ursúa et al. [34] have predicted, using computational methods, the binding affinities for agonists and antagonists in modeled rat and human D2 dopamine receptor, having suggested the importance of Ser193, Ser194 and Ser197 (Ser192, Ser193 and Ser196 in D3R). Kortagere et al. [42], in a recent publication using site-directed mutagenesis and homology modeling studies, have showed that Ser192 in TM5 seems to be crucial for receptor interaction and activation by a ligand through hydrogen bonding with its hydroxyl group. We have demonstrated here the strong attractive interaction of Ser192, Ser193 and Phe188 with eticlopride, and the relative weakness of the interaction with Ser196. In the same way, our data shows the attractive profile of Phe346, Phe106, Phe188, Val189 and Trp342 and the repulsive interactions of Cys114, Ser182 and Val82, which are in agreement with results from Kalani et al. [36], who argued that Phe110, Cys118, Phe189, Val190, Trp386 and Phe390 (Phe106, Cys114, Phe188, Val189, Trp342 and Phe346 in D3R, respectively) are crucial for ligand-binding in modeled D2R structures. Moreover, the understanding of the binding interactions has been useful in approaches as to the prediction of the structure of de D2R in complex with eticlopride, as performed by Obiol-Pardo et al. [18], which used information about the salt bridge formed by Asp110 and the tertiary amine group, the formation of intracellular hydrogen interactions and a more precise evaluation of the ligand energy on binding to predict plausible models of eticlopride binding through docking methodology. Our results also provide information about the individual residues contribution, making useful the description of the binding pocket energy and its interactions with ligands, to further studies in search of new and more potent antipsychotic agents with fewer side effects.

Conclusion

In the last decade, consensus was reached that the understanding of dopamine antagonism is extremely necessary to the development of new more efficient drugs with less adverse effects. In the present study, we analyzed the crystallographic structure D3R-eticlopride via a quantum method, establishing the behavior of the total interaction energy as a function of the binding pocket radius. Considering the range of amino acid residues implicated with the eticlopride binding, we highlighted the significant energy contribution of Asp110, and demonstrated for the first time the participation of Val107, Ser182, Phe188, Val82 and Asn185 on this binding. The present theoretical approach is useful for future studies on the influence of mutated amino acid residues in the binding site using *in silico* simulations through the virtual replacement of residues followed by steps of energy minimization and quantum calculation. Moreover, the present data is of interest due to its potential use in biological analysis, such as site-directed mutagenesis studies and assays of binding affinity of different antagonists to D3R and other members of the dopamine receptor family.

Acknowledgments

The authors acknowledge Prof. D.L. Azevedo at the Federal University of Maranhão, where part of the computational calculations was performed using the DMOL3 code. B.S.C. and V.N.F. are senior researchers from the Brazilian National Research Council (CNPq) and acknowledge the financial support received during the development of this work from the Brazilian Research Agency CNPq-INCT-Nano(Bio) Simes, project 573925/2008-9. E.W.S.C. received financial support from CNPq projects 304338/2007-9 and 482051/2007-8. C.G. received financial support from CNPq project 478916/2010-8.

References

1. Wildenauer DB (2009) Dissecting the Molecular Causes of Schizophrenia. In: Molecular Biology of Neuropsychiatric Disorders, Wildenauer DB (Ed), Springer, Berlin.
2. Inta D, Meyer-Lindenberg A, Gass P (2011) Alterations in Postnatal Neurogenesis and Dopamine Dysregulation in Schizophrenia: A Hypothesis. Schizophr Bull 37: 674-680.
3. Weinberger DR (1987) Implications of Normal Brain Development for the Pathogenesis of Schizophrenia. Arch Gen Psychiatry 44: 660-669.
4. Davie CA (2008) A review of Parkinson's disease. Br Med Bull 86: 109-127.
5. Fahn S (2008) The history of dopamine and levodopa in the treatment of Parkinson's disease. Mov Disord 23: S497-S508.
6. Snyder SH (1976) The dopamine hypothesis of schizophrenia: focus on the dopamine receptor. Am J Psychiatry 133: 197-202.
7. Howes OD, Kapur S (2009) The Dopamine Hypothesis of Schizophrenia: Version III—The Final Common Pathway. Schizophr Bull 35: 549-562.
8. Missale C, Nash SR, Robinson SW, Jaber M, Caron MG (1998) Dopamine Receptors: From Structure to Function. Physiol Rev 78: 189-225.
9. Callier S, Snapyan M, Le Crom S, Prou D, Vincent JD, et al. (2003) Evolution and cell biology of dopamine receptors in vertebrates. Biol Cell 95: 489-502.
10. Giros B, Sokoloff P, Martres MP, Riou JF, Emorine LJ, et al. (1989) Alternative splicing directs the expression of two D2 dopamine receptor isoforms. Nature 342: 923-926.
11. Strange PG (2001) Antipsychotic Drugs: Importance of Dopamine Receptors

for Mechanisms of Therapeutic Actions and Side Effects. Pharmacol Rev 53: 119-133.

12. Stahl SM (2003) Describing an Atypical Antipsychotic: Receptor Binding and Its Role in Pathophysiology. J Clin Psychiatry 5: 9-13.
13. Kapur S, Seeman P (2001) Does Fast Dissociation From the Dopamine D(2) Receptor Explain the Action of Atypical Antipsychotics?: A New Hypothesis. Am J Psychiatry 158: 360-369.
14. Meltzer HY (1999) The Role of Serotonin in Antipsychotic Drug Action. Neuropsychopharmacology 21: 106S-115S.
15. Newman-Tancredi A, Kleven MS (2011) Comparative pharmacology of antipsychotics possessing combined dopamine D2 and serotonin 5-HT1A receptor properties. Psychopharmacology (Berl) 216: 451-473.
16. Martelle JL, Nader MA (2008) A Review of the Discovery, Pharmacological Characterization, and Behavioral Effects of the Dopamine D2-Like Receptor Antagonist Eticlopride. CNS Neurosci Ther 14: 248-262.
17. Chien EY, Liu W, Zhao Q, Katritch V, Han GW, et al. (2010) Structure of the Human Dopamine D3 Receptor in Complex with a D2/D3 Selective Antagonist. Science 330: 1091-1095.
18. Obiol-Pardo C, López L, Pastor M, Selent J (2011) Progress in the structural prediction of G protein-coupled receptors: D3 receptor in complex with eticlopride. Proteins 79: 1695-1703.
19. Hohenberg P, Kohn W (1964) Inhomogeneous Electron Gas. Phys Rev 136: B864-B871.
20. Kohn W, Sham LJ (1965) Self-Consistent Equations Including Exchange and Correlation Effects. Phys Rev 140: A1133–A1138.
21. Gordon MS, Fedorov DG, Pruitt SR, Slipchenko LV (2012) Fragmentation Methods: A Route to Accurate Calculations on Large Systems. Chem Rev 112: 632-672.
22. He X, Zhang JZ (2005) A new method for direct calculation of total energy of protein. J Chem Phys 122: 31103.
23. Zhang DW, Zhang JZ (2003) Molecular fractionation with conjugate caps for full quantum mechanical calculation of protein--molecule interaction energy. J Chem Phys 119: 3599-3605.
24. Chen X, Zhang Y, Zhang JZ (2005) An efficient approach for ab initio energy calculation of biopolymers. J Chem Phys 122: 184105.
25. Gao AM, Zhang DW, Zhang JZH, Zhang Y, (2004) An efficient linear scaling method for ab initio calculation of electron density of proteins. Chem Phys Lett 394: 293-297.
26. Matta CF (2010) Quantum Biochemistry. Wiley-VCH, Germany.
27. Zhou T, Huang D, Caflisch A (2010) Quantum Mechanical Methods for Drug Design. Curr Top Med Chem 10: 33-45.
28. Raha K, Peters MB, Wang B, Yu N, Wollacott AM, et al. (2007) The role of quantum mechanics in structure-based drug design. Drug Discov Today 12: 725-731.
29. Santos SG, Santana JV, Maia FF Jr, Lemos V, Freire VN, et al. (2008) Adsorption of Ascorbic Acid on the C60 Fullerene. J Phys Chem B 112: 14267-14272.
30. Hadad A, Azevedo DL, Caetano EWS, Freire VN, Mendonça GLF, et al. (2011) Two-Level Adsorption of Ibuprofen on C60 Fullerene for Transdermal Delivery: Classical Molecular Dynamics and Density Functional Theory Computations. J Phys Chem C 115: 24501-24511.
31. da Costa RF, Freire VN, Bezerra EM, Cavada BS, Caetano EW, et al. (2012) Explaining statin inhibition effectiveness of HMG-CoA reductase by quantum biochemistry computations. Phys Chem Chem Phys 14: 1389-1398.
32. Delley B (1990) An all-electron numerical method for solving the local density functional for polyatomic molecules. J Chem Phys 92: 508-517.
33. Delley B (2000) From molecules to solids with the DMol[sup 3] approach. J Chem Phys 113: 7756-7764.
34. Soriano-Ursúa MA, Ocampo-López JO, Ocampo-Mendoza K, Trujillo-Ferrara JG, Correa-Basurto J (2011) Theoretical study of 3-D molecular similarity and ligand binding modes of orthologous human and rat D2 dopamine receptors. Comput Biol Med 41: 537-545.
35. Hu L, Eliasson J, Heimdal J, Ryde U (2009) Do Quantum Mechanical Energies Calculated for Small Models of Protein-Active Sites Converge? J Phys Chem A 113: 11793-11800.
36. Kalani MY, Vaidehi N, Hall SE, Trabanino RJ, Freddolino PL, et al. (2004) The predicted 3D structure of the human D2 dopamine receptor and the binding site and binding affinities for agonists and antagonists. Proc Natl Acad Sci USA 101: 3815-3820.
37. Javitch JA, Fu D, Chen J (1996) Differentiating dopamine D2 ligands by their sensitivities to modification of the cysteine exposed in the binding-site crevice. Mol Pharmacol 49: 692-698.
38. Boeckler F, Gmeiner P (2006) The structural evolution of dopamine D3 receptor ligands: Structure-activity relationships and selected neuropharmacological aspects. Pharmacol Ther 112: 281-333.
39. Tschammer N, Elsner J, Goetz A, Ehrlich K, Schuster S, et al. (2011) Highly Potent 5-Aminotetrahydropyrazolopyridines: Enantioselective Dopamine D3 Receptor Binding, Functional Selectivity, and Analysis of Receptor-Ligand Interactions. J Med Chem 54: 2477-2491.
40. de Paulis T, Kumar Y, Johansson L, Rämsby S, Florvall L, et al. (1985) Potential neuroleptic agents. 3. Chemistry and antidopaminergic properties of substituted 6-methoxysalicylamides. J Med Chem 28: 1263-1269.
41. Saran A, Coutinho E (1994) Quantum mechanical calculations on dopamine D2-receptor antagonists: Conformation of remoxipride, eticlopride and NCQ 115. Chem Sci 106: 149-161.
42. Kortagere S, Cheng SY, Antonio T, Zhen J, Reith ME, et al. (2011) Interaction of novel hybrid compounds with the D3 dopamine receptor: Site-directed mutagenesis and homology modeling studies. Biochem Pharmacol 81: 157-163.